

## Positronium quenching via collisions with triplet states of photomagnetic molecules

C. I. Eom,\* S. V. Naidu,<sup>†</sup> S. C. Sharma, and J. M. Kowalski<sup>‡</sup>

*Department of Physics, Center for Positron Studies, The University of Texas at Arlington, Arlington, Texas 76019*

(Received 14 May 1990)

We have studied positronium quenching resulting from collisions with the triplet states of benzaldehyde, oxygen, benzophenone, and bromonaphthalene. Positronium pick-off decay rates are presented as functions of triplet populations via uv irradiation of benzaldehyde-ethane, benzaldehyde-helium, and oxygen-ethane gaseous mixtures and of benzophenone and bromonaphthalene adsorbed porous silicas. Our results show that the cross sections for positronium quenching in collisions with excited triplet states are not as high as reported previously. The oxygen data suggest reactions between "hot" (nonthermal) positronium and oxygen molecules.

### I. INTRODUCTION

The experiments by Brandt in 1977 suggested that uv illumination of Ar, N<sub>2</sub>, and air containing trace amounts of SO<sub>2</sub> or benzaldehyde quenched positronium with quenching cross sections of the order of  $10^3\pi a_0^2$  as a result of spin conversion through positronium interactions with excited triplet states.<sup>1</sup> These results suggested intriguing possibilities of using positronium to study the role of excited triplet states in photosynthesis and energy transport in biologically important processes and also posed new questions about the scattering of leptonic atoms from excited electronic states of matter. However, these first experiments suffered from several limitations. Specifically the density of the carrier gas was mainly  $2.45 \times 10^{19}$  molecules/cm<sup>3</sup> which could not stop a sufficient number of energetic positrons in the medium under study, and therefore Ps formation efficiency was very low. The concentration of the triplet-state molecules  $C_T$  was limited from  $2 \times 10^{-8}$  to  $1 \times 10^{-7}$ . The measurements were performed only at four different values of  $C_T$  for benzaldehyde and three different values of  $C_T$  for SO<sub>2</sub>, and the total number of counts under the lifetime spectrum was of the order of  $10^4$ , which was not enough to accurately resolve the long-lived orthopositronium (*o*-Ps) component from the lifetime spectrum. Consequently, Brandt's method of analysis was to integrate the lifetime spectrum after a certain time  $t_c$  ( $\sim 30$  ns), and this precluded detailed information about the lifetimes and relative intensities of the different components present in the spectrum. The main findings of these experiments were that the photoexcited triplet-state molecules quenched long-lived *o*-Ps dominantly via spin-flip processes with quenching cross sections of  $680\pi a_0^2$  for SO<sub>2</sub> and  $1100\pi a_0^2$  for benzaldehyde. These cross sections are dramatically large compared to the other known values of Ps-quenching cross sections for gaseous media. For example, the *o*-Ps-quenching cross sections are known to be  $1.3 \times 10^{-5}\pi a_0^2$  for N<sub>2</sub>,  $1.1 \times 10^{-3}\pi a_0^2$  for O<sub>2</sub>, and  $28\pi a_0^2$  or NO<sub>2</sub>.

In this paper we present results from a detailed study of the interactions of Ps with triplet states of several pho-

tomagnetic molecules based on more precise data and improved data analysis. In the experiments with ethane-benzaldehyde mixtures, ethane gas was used to enhance Ps formation probability (Ps yields in ethane vary from  $0.41 \pm 0.03$  at low densities to  $\sim 0.8$  at high densities<sup>2,3</sup>), and the benzaldehyde photomagnetic molecules were introduced into this medium at concentrations ranging from  $10^{-8}$  to  $10^{-4}$ . Experiments were also performed with helium-benzaldehyde mixtures in order to examine whether possible energy loss by the excited triplet states ( $T^*$ ) of benzaldehyde via rotational or vibrational excitations of the ethane molecules had any effect on the positron lifetime spectra. To study any possible differences between the interactions of positronium with the excited and ground states of triplet molecules, O<sub>2</sub> molecules, which are triplet in their ground states, were used with high-pressure ethane gas. Several samples were specially prepared for data collection in the solid phase. Contrary to the gaseous samples, these solid samples exhibit phosphorescence in the visible part of the spectrum.<sup>4,5</sup> They thus provide a convenient "tool" to definitely assure the existence of the excited triplet states in the medium. The improvements incorporated in the present experiments can be summarized as follows. (a) We have chosen ethane as a buffer gas in the mixtures because ethane is now known to provide a very high positronium yield of 50–80% in gases.<sup>2</sup> This obviously enables good statistics for the orthopositronium component in the lifetime spectrum without long accumulation times. (b) We collected approximately  $10^6$  counts under each lifetime spectrum. This enabled the resolution of the lifetime spectrum into three components with relatively high precision. (c) We have extended measurements to much wider ranges of triplet concentrations. (d) We have conducted experiments with several solid samples which were prepared by adsorbing photomagnetic molecules within the pore network of silica gel samples. With known phosphorescent deexcitation in the visible range these samples provided conclusive evidence in support of our findings with the gaseous samples. (e) We have made measurements of Ps quenching with the triplet states of O<sub>2</sub>. In addition to reproducing the well-known high-Ps-quenching cross sections, these latter experiments also provided new results.

These improvements have enabled us to present detailed results based on a systematic study of Ps quenching in collisions with triplet states of molecules.

Following discussion in Sec. II of the apparatus and the techniques of the data collection and analysis, we discuss the theoretical background in Sec. III. The results are presented and discussed in Sec. IV.

## II. EXPERIMENTAL DETAILS

### Gas-handling system and gas sample

A schematic of the gas-handling system is shown in Fig. 1. A 3.0-in-wide and 6.0-in-deep cylinder made of 316 stainless steel was used for the mixing chamber. Several stainless-steel tubings of 0.5-in inner diam were welded to the mixing chamber. One of the tubings was connected to the main chamber through two valves. All of the joints in the system utilized silver-plated gaskets for ultra-high vacuum as well as for high pressure, which also made it possible to separate each joint from the system for cleaning, or replacement of parts, or for some necessary changes in the system. Among the other tubings, one was directly connected to the diffusion pump, the other was connected to the stainless-steel-Pyrex test tube which contained phosphor chemical. One of the other remaining tubings was connected to the host gas ( $C_2H_6$ , He, etc.) container through an  $O_2$  purifier, while the others were connected to the vacuum and high-pressure gauges, respectively. The main chamber had 1.5-in inner diam and 1.5-in inner height and was made of the same stainless steel. This main chamber was equipped with two 0.34-in-diam sapphire optical windows, and it was connected to the vacuum and high-pressure gauges passing through the chamber. The positron source assembly was held at the ceiling of the chamber, 0.17 in away from the center so that the uv light rays would not intersect with the source.

The entire gas-handling system was prepared for induction of the gas sample by utilizing the standard baking and flushing techniques. After a thorough initial cleaning and pressure-leak testing, a diffusion pump was used to evacuate the whole system while all the tubings and chambers were heated. This was done many times for several days in order to purge the system of any im-

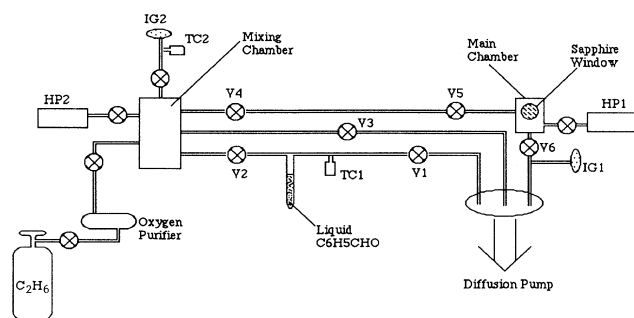


FIG. 1. Schematic of the gas-handling system. TC=thermocouple gauge, IG=ionization gauge, HP=high-pressure gauge, V=valves.

purities. After reaching the equilibrium pressure ( $\sim 10^{-6}$  torr), about  $5 \text{ cm}^3$  of liquid-benzaldehyde sample was introduced to the stainless-steel-Pyrex test tube. With the other parts of the system isolated (which means that with valves, 2, 3, and 6 closed and valve 1 open in Fig. 1) the test tube was evacuated first at room temperature for several minutes to get rid of most of the air and then cooled down to 77 K in order to reduce the vapor pressure of benzaldehyde while evacuating. This procedure was repeated several times and then valve (V1) was closed to isolate the benzaldehyde section from the rest of the system. After obtaining a vacuum of the order of  $10^{-6}$  torr in the rest of the system, benzaldehyde vapor was loaded into the mixing chamber to a pressure of about 0.1–1000 mTorr. This low-pressure gas was then mixed with the high-pressure ( $\sim 300$  psi) host gas (e.g.,  $C_2H_6$ ). Finally, this mixture with the known concentration of benzaldehyde was brought to the main chamber for the collection of the lifetime spectrum. With this procedure, we were able to mix ethane and benzaldehyde to obtain benzaldehyde concentrations of the order of  $\sim 10^{-4}$  to  $10^{-8}$ . The gases used were 99.99% pure ethane (helium and oxygen) and the vapor of liquid benzaldehyde was greater than 99% pure.

### uv source and detection system

Figure 2 shows the uv source and detection system. The uv source was a 200-W mercury-arc lamp system (Oriol Model No. 66006) which includes lamp housing with focusing lens, igniter, and a high-voltage power supply. A 5-in-long Pyrex cylinder-filled with distilled water was placed in front of the mercury lamp to absorb the infrared rays. An ESCO 7-59 Corning filter or S1-uv filter, which transmits only ultraviolet, was placed next to the ir absorber. A monochromator was used to select the excitation wavelength for the  $S_0 \rightarrow S_1$  transition of the phosphor molecule. To vary the intensity of the incident uv several fused silica neutral density filters were used separately. The intensity of incident uv was monitored by measuring the intensity of the beam reflected by a partial mirror. Oriol Model No. 7070 photometer was used with a RCA 1P21 photomultiplier tube (PMT) for uv-intensity measurement. In most cases, the intensity of transmitted uv was also measured by another photometer (Pacifc Photometric Instruments Model No. 124) employing RCA 1P21 PMT.

The positron lifetime spectra were measured by employing a standard fast-fast timing spectrometer with a

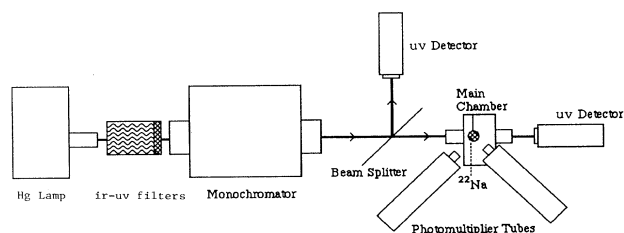


FIG. 2. Schematic of the uv source and the detection system.

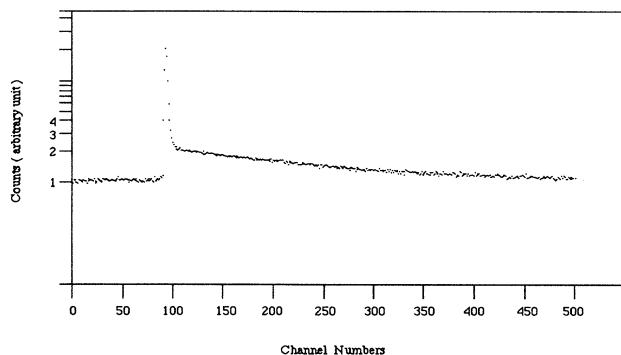


FIG. 3. A typical lifetime spectrum. The longest-lived component is clearly visible.

FWHM of about 0.4 ns for the  $^{60}\text{Co}$  resolution data and with a time calibration of about 0.082 ns/channel. These spectra were resolved into three exponential components by using POSITRONFIT EXTENDED.<sup>6</sup> The longest-lived component, with an average decay rate  $\lambda_{o\text{-Ps}}$ , arises from the pick-off annihilations of orthopositronium, the shortest-lived component represents contributions from the annihilations of parapositronium and of positrons at the walls of the metallic sample chamber, and the intermediate component, with an average decay rate  $\lambda$ , arises from the annihilations of free positrons.<sup>7</sup> Each lifetime spectrum contained approximately  $10^6$  counts. A typical lifetime spectrum is shown in Fig. 3 in which the longest-lived component is clearly resolved. Additional details about the collection and analysis of the positron lifetime spectra in gases have been discussed elsewhere.<sup>8</sup>

### III. THEORETICAL BACKGROUND

#### The excited triplet state

The basic mechanisms for producing metastable excited states of photomagnetic molecules, like benzaldehyde ( $\text{C}_6\text{H}_5\text{CHO}$ ), are well known.<sup>9,10</sup> Although a direct transition from an electronic singlet ground state ( $S_0$ ) to an excited triplet state ( $T_1^*$ ) of the molecule by photon absorption is forbidden, a triplet state can be populated indirectly through spin-orbit coupling. The processes involved in the population and subsequent deexcitation of the triplet state are shown in Fig. 4. These include (1)  $S_0 \rightarrow S_n$ , a transition from the singlet ground state to one of the vibrational excited states of the  $n$ th singlet excited state as a result of photon absorption; (2) vibrational relaxation to the lowest vibrational level of  $S_n$  (3) internal conversion, a transition from the lowest vibrational level of  $S_n$  to the isoenergetic vibrational level of a lower electronic state,  $S_{n-1}$  (by successive internal conversion and vibrational relaxation the molecule deactivates rapidly to  $S_1$ ); (4) fluorescence, a rapid decay (lifetime  $\sim 10^{-11}$ s) from  $S_1$  to  $S_0$ ; (5) intersystem crossing, a transition from  $S_1$  to one of the vibrational levels of the excited triplet state as a result of spin-orbit coupling. The molecule then undergoes transition to the lowest vibrational state of the triplet state via internal conversion and vibrational relaxation. The eventual transition  $T_1^* \rightarrow S_0$  may be

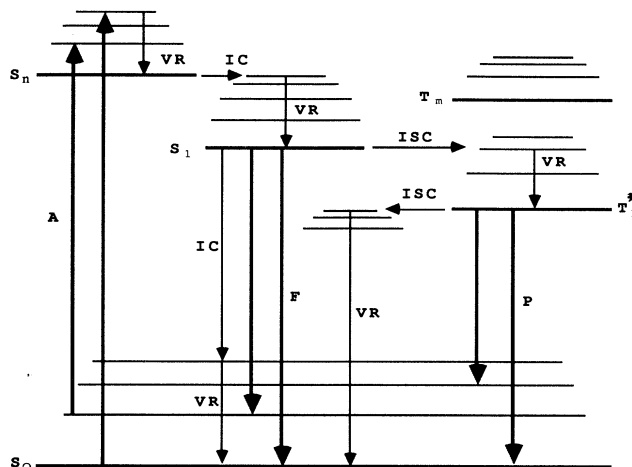


FIG. 4. Schematic of the energy level diagram for a photomagnetic molecule.  $S$  and  $T$  represent singlet and triplet states, respectively.  $T_1^*$  is the lowest excited triplet state that decays via phosphorescence ( $P$ ) to the singlet ground state.

completed either by radiationless deactivation or by phosphorescence that involves emission of a photon. The lifetime of the metastable excited triplet state depends on the surrounding medium and can be varied from  $10^{-3}$  to several seconds. A relatively long lifetime ( $\sim 50$  ns) and a high mobility of the orthopositronium atom at the pressure and temperature conditions of the present experiments coupled with a long lifetime of the excited triplet state should make it possible to study the interactions between positronium and the triplet state.

Following Brandt,<sup>1</sup> we discuss the main theoretical arguments and modify Brandt's results to include nonlinear effects that become important at high triplet concentrations reached in our experiments. The nonlinear effects may become important in a variety of different experiments (e.g., liquid solutions, gas mixtures, etc.) in which positronium quenching is studied at sufficiently high concentrations of the quenching agents.<sup>11</sup> Let  $n_o(x, t)$  denote the probability of an  $o\text{-Ps}$  formed at  $t=0$  and at depth  $x$  in the sample to survive until time  $t$ , and  $n_p(x, t)$  denote the corresponding quantity for parapositronium ( $p\text{-Ps}$ ). One can then express the rates of change in the probabilities as follows:

$$\dot{n}_o(x, t) = -[\lambda_o + k_o(x)]n_o(x, t) + k_p(x)n_p(x, t), \quad (1)$$

$$\dot{n}_p(x, t) = -[\lambda_p + k_p(x)]n_p(x, t) + k_o(x)n_o(x, t), \quad (2)$$

where  $\lambda_o$  = effective  $o\text{-Ps}$  annihilation rate =  $\lambda_{v,o} + \lambda_{m,o}$ ,  $\lambda_{v,o}$  =  $o\text{-Ps}$  annihilation rate in vacuum,  $\lambda_{m,o}$  =  $o\text{-Ps}$  quenching rate in medium,  $\lambda_p$  = effective  $p\text{-Ps}$  annihilation rate =  $\lambda_{v,p} + \lambda_{m,p}$ ,  $\lambda_{v,p}$  =  $p\text{-Ps}$  annihilation rate in vacuum,  $\lambda_{m,p}$  =  $p\text{-Ps}$  quenching rate in medium,  $k_o$  = ortho-to-para conversion rate,  $k_p$  = para-to-ortho conversion rate.

The initial conditions are  $n_o(x, 0) = \frac{3}{4}\beta$  and  $n_p(x, 0) = \frac{1}{4}\beta$ , where  $\beta$  denotes the Ps yield in the medium. The solutions of the above equations are

$$n_o(x,t) = \frac{3}{4}\beta \left[ \frac{\Gamma_2(x) - \Gamma_o(x) + \frac{1}{3}k_p(x)}{\Gamma_2(x) - \Gamma_1(x)} e^{-\Gamma_1(x)t} + \frac{\Gamma_1(x) - \Gamma_o(x) + \frac{1}{3}k_p(x)}{\Gamma_1(x) - \Gamma_2(x)} e^{-\Gamma_2(x)t} \right] \quad (3)$$

and

$$n_p(x,t) = \frac{1}{4}\beta \left[ \frac{\Gamma_2(x) - \Gamma_p(x) + 3k_o(x)}{\Gamma_2(x) - \Gamma_1(x)} e^{-\Gamma_1(x)t} + \frac{\Gamma_1(x) - \Gamma_p(x) + 3k_o(x)}{\Gamma_1(x) - \Gamma_2(x)} e^{-\Gamma_2(x)t} \right] \quad (4)$$

with the abbreviations  $\Gamma_{o,p} \equiv \lambda_{o,p} + k_{o,p}(x)$ . The disappearance rates are given by

$$\Gamma_{1,2} = \frac{1}{2} \{ \lambda_p + \lambda_o + k_p(x) + k_o(x) \pm \sqrt{[\lambda_p - \lambda_o + k_p(x) - k_o(x)]^2 + 4k_p(x)k_o(x)} \}, \quad (5)$$

where the subscripts 1 and 2 refer to the + and - signs, respectively. When the conversion rates are much lower than the the annihilation rates, i.e.,  $k_{o,p} \ll \lambda_{o,p}$ , the expressions for  $\Gamma_{1,2}$  can be simplified to  $\Gamma_1 = \lambda_p + k_p(x)$ ,  $\Gamma_2 = \lambda_o + k_o(x)$ .

Ps lifetime spectrum is then represented by

$$n_{Ps}(x,t) = \beta [I_1(x)e^{-\Gamma_1(x)t} + I_2(x)e^{-\Gamma_2(x)t}],$$

where

$$I_1(x) = \frac{\Gamma_2(x) - \lambda}{\Gamma_2(x) - \Gamma_1(x)}, \quad I_2(x) = \frac{\Gamma_1(x) - \lambda}{\Gamma_1(x) - \Gamma_2(x)}, \quad (6)$$

$$\lambda = \frac{1}{4}\lambda_p + \frac{3}{4}\lambda_o.$$

Photon-induced changes in  $\Gamma_2$  and  $I_2$  can be measured to yield

$$\frac{\Delta\Gamma_2}{\Gamma_2^{\text{off}}} = \frac{k_o}{\lambda_o}$$

and

$$\frac{I_2^{\text{off}}}{\Delta I_2} = \frac{\Delta\Gamma_1}{\Gamma_1^{\text{off}} - \lambda} = \frac{4}{3} \frac{k_p}{\lambda_p - \lambda_o}, \quad (7)$$

where

$$\Delta\Gamma_{1,2} = \Gamma_{1,2}^{\text{on}} - \Gamma_{1,2}^{\text{off}}, \quad \Gamma_{1,2}^{\text{on}} = \lambda_{p,o} + k_{p,o},$$

$$\Gamma_{1,2}^{\text{off}} = \lambda_{p,o}, \quad \Delta I_2 = I_2^{\text{on}} - I_2^{\text{off}}.$$

In case  $k_{o,p} \ll \lambda_{o,p}$ ,

$$I_2^{\text{on}} = I_2^{\text{off}} \frac{\Gamma_1^{\text{on}} - \lambda}{\Gamma_1^{\text{off}} - \lambda};$$

and therefore

$$\begin{aligned} \frac{k_p}{k_o} &= \frac{\sigma_{p-Ps}}{\sigma_{o-Ps}} \approx \frac{3}{4} \frac{\Delta I_2}{I_2^{\text{off}}} \frac{\Gamma_2^{\text{off}}}{\Delta\Gamma_2} \left[ \frac{\lambda_p}{\lambda_o} - 1 \right] \\ &= \frac{3}{4} \frac{\Delta I_2}{I_2^{\text{off}}} \frac{(\lambda_p - \Gamma_2^{\text{off}})}{\Delta\Gamma_2}. \end{aligned} \quad (8)$$

Here "on" and "off" refer to the experimental conditions of the uv lamp being on and off, respectively. From the measured values of *o*-Ps annihilation parameters, one can thus obtain the ratio  $\sigma_{p-Ps}/\sigma_{o-Ps}$ , which depends on the relative magnitudes of the spin-flip and electron-exchange

cross sections.

Suppose a gas contains a small concentration *C* of molecules or atoms in electronic singlet ground state (*S* = 0). Light of frequency  $\omega$  and intensity  $L_o(\omega)$  enters at  $x=0$  and populates metastable paramagnetic triplet states  $T^*$  (*S* = 1). At depth  $x$ , the light produces a steady-state concentration  $C_T(x,\omega) < C$ . Assuming that Lambert-Beer's law is valid,  $C_T$  is given by

$$C_T = C \frac{\phi_T \tau_T \epsilon(\omega) L_o(\omega) \exp[-\epsilon(\omega)CNx]}{1 + \phi_T \tau_T \epsilon(\omega) L_o(\omega) \exp[-\epsilon(\omega)CNx]}, \quad (9)$$

where  $\phi_T$  is the triplet formation efficiency,  $\tau_T$  is the triplet lifetime,  $\epsilon(\omega)$  is the photoabsorption cross section which is proportional to the extinction coefficient,  $L_o(\omega)$  is the intensity of light at frequency  $\omega$ , and  $N$  is the density of inert diamagnetic molecules. When  $C_T(x,\omega) \ll C$ ,

$$C_T(x,\omega) = C \phi_T \tau_T \epsilon(\omega) L_o(\omega) \exp[-\epsilon(\omega)CNx]. \quad (10)$$

As Ps and  $T^*$  interact, *p*-Ps is quenched at the rate  $k_p(x,\omega)$  and *o*-Ps at the rate  $k_o(x,\omega)$ . Assuming that spin conversion changes *p*-Ps to *o*-Ps and *o*-Ps to *p*-Ps with efficiencies  $\alpha_p$  and  $\alpha_o$ , respectively,

$$k_p(x,\omega) = \alpha_p \nu_T N C_T(x,\omega) = \sigma_{p-Ps} V N C_T(x,\omega), \quad (11)$$

$$k_o(x,\omega) = \alpha_o \nu_T N C_T(x,\omega) = \sigma_{o-Ps} V N C_T(x,\omega).$$

The volume rate,  $\nu_T = \sigma_T V$ , depends on the thermal Ps velocity  $V$  and the spin interaction cross section  $\sigma_T$ . We define  $\sigma_{p-Ps} = \alpha_p \sigma_T$  and  $\sigma_{o-Ps} = \alpha_o \sigma_T$ . We set  $\Gamma_1 \equiv \lambda_{p-Ps}$ ,  $\Gamma_2 \equiv \lambda_{o-Ps}$ ,  $\lambda_p \equiv \lambda_{p-Ps}^{\text{off}}$  and  $\lambda_o \equiv \lambda_{o-Ps}^{\text{off}}$ . Without any light, the annihilation rates of *p*-Ps and *o*-Ps are given by  $\lambda_{p-Ps}^{\text{off}}$  and  $\lambda_{o-Ps}^{\text{off}}$ , respectively. The rates under illumination become

$$\lambda_{p-Ps} = \lambda_{p-Ps}^{\text{off}} + k_p(x,\omega), \quad (12)$$

$$\lambda_{o-Ps} = \lambda_{o-Ps}^{\text{off}} + k_o(x,\omega).$$

When there are no photomagnetic impurities in the system, the rates of change in the number of free positrons, orthopositroniums, and parapositroniums with time are expressed by the following equations:

$$\dot{n}_f(t) = -[\lambda_f + W(f \rightarrow o) + W(f \rightarrow p)]n_f(t),$$

$$\dot{n}_o(t) = W(f \rightarrow o)n_f(t) - (\lambda_{v,o} + \lambda_{m,o})n_o(t),$$

$$\dot{n}_p(t) = W(f \rightarrow p)n_f(t) - (\lambda_{v,p} + \lambda_{m,p})n_p(t),$$

where  $\lambda_f$  = free positron annihilation rate,  $W(f \rightarrow o)$  = free to *o*-Ps conversion rate,  $W(f \rightarrow p)$  = free to *p*-Ps conversion rate,  $n_f(t)$  = number of free positrons at time *t*,  $n_o(t)$  = number of *o*-Ps at time *t*, and  $n_p(t)$  = number of *p*-Ps at time *t*. The effective annihilation rates can be written as

$$\begin{aligned}\lambda_f^{\text{eff}} &= \lambda_f + W(f \rightarrow o) + W(f \rightarrow p), \\ \lambda_o^{\text{eff}} &= \lambda_{v,o} + \lambda_{m,o}, \\ \lambda_p^{\text{eff}} &= \lambda_{v,p} + \lambda_{m,p}.\end{aligned}\quad (13)$$

In the following, we extend this model to include the nonlinear effects that become important at sufficiently high values of  $C_T$ . In the presence of the triplet states, the population equations can be expressed in terms of the decay matrix  $\hat{D}$ ,

$$\begin{bmatrix} \dot{n}_f(t) \\ \dot{n}_o(t) \\ \dot{n}_p(t) \end{bmatrix} = \hat{D} \begin{bmatrix} n_f(t) \\ n_o(t) \\ n_p(t) \end{bmatrix},$$

where

$$\hat{D} = \begin{bmatrix} -\lambda_f^{\text{eff}} & 0 & 0 \\ W(f \rightarrow o) & -\lambda_o^{\text{eff}} - W(o \rightarrow p)C_T & W(p \rightarrow o)C_T \\ W(f \rightarrow p) & W(o \rightarrow p)C_T & -\lambda_p^{\text{eff}} - W(p \rightarrow o)C_T \end{bmatrix} \quad (14)$$

and  $W(o \rightarrow p)$  = ortho-to-para positronium conversion rate and  $W(p \rightarrow o)$  = para-to-ortho positronium conversion rate. A solution of these equations provides the following three eigenvalues:

$$\begin{aligned}\sigma_1 &= -\lambda_f^{\text{eff}}, \\ \sigma_{2,3} &= \frac{1}{2} \{ -\lambda_p^{\text{eff}} - \lambda_o^{\text{eff}} - C_T [W(p \rightarrow o) + W(o \rightarrow p)] \} \\ &\quad \pm \frac{1}{2} \sqrt{ \{ \lambda_p^{\text{eff}} - \lambda_o^{\text{eff}} + C_T [W(p \rightarrow o) - W(o \rightarrow p)] \}^2 + 4C_T^2 W(p \rightarrow o)W(o \rightarrow p) }.\end{aligned}\quad (15)$$

Now the solutions for the *o*-Ps component can be approximated by

$$n_o(t) \approx Ge^{\sigma_2 t},$$

where

$$\begin{aligned}G &= \frac{-n_f(0) \frac{\alpha}{\delta} + n_f(0) \frac{C_T W(p \rightarrow o)}{\lambda_{o\text{-Ps}}^{\text{eff}} + C_T W(o \rightarrow p) + \sigma_2} \frac{\beta}{\delta}}{1 - \gamma}, \\ \alpha &= W(f \rightarrow o)(\lambda_p^{\text{eff}} + \lambda_f^{\text{eff}}) + C_T W(p \rightarrow o)[W(f \rightarrow o) + W(f \rightarrow p)], \\ \beta &= W(f \rightarrow p)(\lambda_o^{\text{eff}} + \lambda_f^{\text{eff}}) + C_T W(o \rightarrow p)[W(f \rightarrow o) + W(f \rightarrow p)], \\ \gamma &= \frac{C_T^2 W(o \rightarrow p)W(p \rightarrow o)}{[\lambda_{o\text{-Ps}}^{\text{eff}} + C_T W(o \rightarrow p) + \sigma_2][\lambda_{p\text{-Ps}}^{\text{eff}} + C_T W(p \rightarrow o) + \sigma_1]},\end{aligned}\quad (16)$$

and

$$\delta = [\lambda_o^{\text{eff}} + C_T W(o \rightarrow p) - \lambda_f^{\text{eff}}][\lambda_p^{\text{eff}} + C_T W(p \rightarrow o) - \lambda_f^{\text{eff}}] - C_T^2 W(p \rightarrow o)W(o \rightarrow p).$$

Assuming

$$\frac{4C_T^2 W(p \rightarrow o)W(o \rightarrow p)}{\{ \lambda_p^{\text{eff}} - \lambda_o^{\text{eff}} + C_T [W(p \rightarrow o) - W(o \rightarrow p)] \}^2} \ll 1,$$

we obtain

$$\begin{aligned}\lambda_{o\text{-Ps}} &= \lambda_{o\text{-Ps}}^{\text{eff}} + C_T W(o \rightarrow p) \\ &\quad - \frac{2C_T^2 W(o \rightarrow p)W(p \rightarrow o)}{\lambda_{p\text{-Ps}}^{\text{eff}} - \lambda_{o\text{-Ps}}^{\text{eff}} + C_T [W(p \rightarrow o) - W(o \rightarrow p)]} \\ &= \lambda_{o\text{-Ps}}^{\text{eff}} + C_T \sigma_{o\text{-Ps}} V N \\ &\quad - \frac{2C_T^2 V^2 N^2 \sigma_{o\text{-Ps}} \sigma_{p\text{-Ps}}}{\lambda_{p\text{-Ps}}^{\text{eff}} - \lambda_{o\text{-Ps}}^{\text{eff}} + C_T V N (\sigma_{p\text{-Ps}} - \sigma_{o\text{-Ps}})}.\end{aligned}\quad (17)$$

Equation (17) shows a parabolic decrease in  $\lambda_{o\text{-Ps}}$  at sufficiently high concentrations of the triplet states. The first two terms are essentially the same as those given in Brandt's theory. The  $C_T^2$  term is an additional contribution that accounts for a competition between para-to-ortho and ortho-to-para conversions. While Brandt's theory predicts a linear increase in  $\lambda_{o\text{-Ps}}$  with increasing  $C_T$ , Eq. (17) predicts a linear increase in  $\lambda_{o\text{-Ps}}$  with  $C_T$  at low concentration, a deviation from this linearity at intermediate  $C_T$ , and a decrease in  $\lambda_{o\text{-Ps}}$  at high enough concentrations of the excited triplet states.

#### IV. RESULTS AND DISCUSSION

##### Effect of uv on positronium decay in pure ethane

In order to see whether the radiation used in these experiments had any effect on positronium quenching in

pure ethane, we first measured positron lifetime spectra in pure ethane gas. Since the energy of a photon of wavelength = 371 nm (the excitation wavelength for the  $S_0 \rightarrow S_1$  transition in benzaldehyde,  $\sim 3.39$  eV) is higher than the rotational and vibrational excitation energies of ethane, the pick-off decay rates of positronium could be altered as a result of positronium collisions with an excited molecule. Positronium decay rates and relative intensities measured in ethane at 23.3 and 53.9 amagat (1 amagat  $\approx 2.7 \times 10^{19}$  molecules  $\text{cm}^{-3}$  at 273 K and 101.3 kPa) as a function of photocurrent are shown in Figs. 5 and 6. The weighted average values of  $\lambda_{o\text{-Ps}} = 0.020 \pm 0.002$  and  $0.030 \pm 0.002$   $\text{ns}^{-1}$  and of  $I_{o\text{-Ps}} = 24.5\%$  and  $39.0\%$  at 23.3 and 53.9 amagat, are in excellent agreement with previous results.<sup>12</sup> These data show that positronium decay is not influenced by uv radiation passing through ethane at these conditions of density and photocurrent. This indicates either (a) there is no absorption of uv by ethane molecules that do not possess a permanent dipole moment, or (b) if uv was absorbed at all, a rapid (the mean lifetime of the excited molecular state  $S_1 \ll o\text{-Ps}$  lifetime) deexcitation should have occurred due to a high frequency of collisions between molecules at these densities.

#### Effects of uv on positronium decay in ethane-benzaldehyde mixtures

Figures 7(a)–7(d) show sets of data for  $\lambda_{o\text{-Ps}}$  versus photocurrent at four ethane densities ranging from 13.5 to 30.9 amagat and benzaldehyde concentrations in the range  $3.3 \times 10^{-6}$  to  $3.7 \times 10^{-5}$ . Contrary to Brandt's results, Fig. 7 shows no variation in  $\lambda_{o\text{-Ps}}$  with increasing photocurrent. Since no variation in  $\lambda_{o\text{-Ps}}$  was observed, we decided to systematically test and eliminate possible sources of discrepancy. In the following, we discuss a number of important tests (without regard to any order of significance) which were performed in order to resolve this apparent discrepancy.

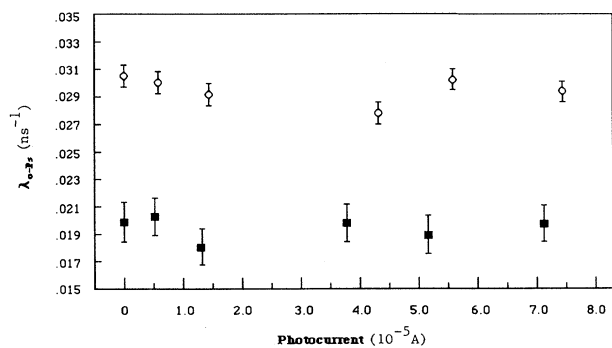


FIG. 5. Pick-off decay rate of  $o\text{-Ps}$  vs photocurrent for pure ethane samples at two different densities (at 23.3 amagat, O at 53.9 amagat).

#### Test No. 1. Are there benzaldehyde molecules in the main chamber?

Benzaldehyde is known to be sticky to the walls of the tubing, mixing chamber, etc. Since we were transferring a small amount of benzaldehyde to the high-vacuum ( $\sim 2 \times 10^{-6}$  torr) mixing chamber, it was possible that the very sticky and heavy ( $\sim 3.5$  times heavier than  $\text{C}_2\text{H}_6$  molecule) benzaldehyde molecules has stuck to the wall of the mixing chamber and tubing. This could have effectively reduced the benzaldehyde concentration in the main chamber. For this reason, to ensure the presence of benzaldehyde molecules, we prepared a mixture of benzaldehyde and ethane and left valve 3 (V3) and valve 6 (V6) open overnight while heating the main chamber, mixing chamber, and transfer tubings to a temperature of about 340 K. This procedure ensures the presence of gaseous benzaldehyde in the main chamber. From the lifetime measurements, made following this heating treatment, no variation in  $\lambda_{o\text{-Ps}}$  was observed as a function of photocurrent. After this series of measurements we released the mixture in the main chamber by removing the top flange. As the mixture escaped, the characteristic smell of benzaldehyde was unambiguously detected verifying the existence of benzaldehyde molecules in the main chamber.

#### Test No. 2: Is the excitation wavelength reaching benzaldehyde molecules in the main chamber?

Since we did not observe any change in  $\lambda_{o\text{-Ps}}$  (Fig. 7) we tested whether excitation wavelengths for benzaldehyde (354, 366, and 371 nm) were passing through the incident optical window into the main chamber. We directed the Hg lamp to one of the optical windows and monitored the intensity of the transmitted uv as a function of wavelength by using a monochromator next to the exit window. The measured spectrum showed several peaks in the 300–400-nm range, which were almost identical to the spectrum of the lamp. It is clear from these data that the excitation radiation at 354, 366, and 371 nm was reaching the benzaldehyde molecules in the main chamber.

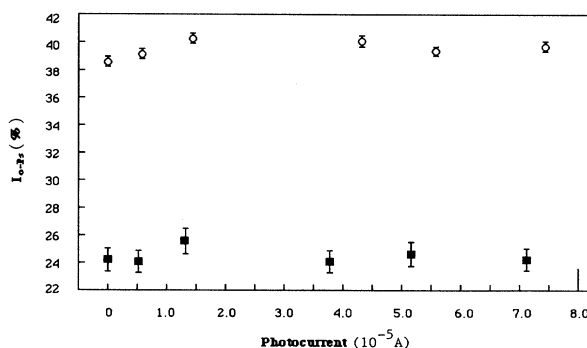


FIG. 6. Relative intensity of the  $o\text{-Ps}$  component vs photocurrent for pure ethane samples at two different densities (at 23.3 amagat, O at 53.9 amagat).

*Test No. 3: Is there  $T^*$  in the main chamber?*

If the scattering cross section between  $o$ -Ps and excited triplet states of benzaldehyde is as large as reported by Brandt, then a measurable change in  $\lambda_{o\text{-Ps}}$  is expected even at the lowest concentration of benzaldehyde used in our experiments. However, our results show no change in  $\lambda_{o\text{-Ps}}$ . It is then possible that the scattering cross section is not large enough to produce the claimed result<sup>1</sup> at such low concentrations. The second term in Eq. (17) becomes significant when  $\sigma_{o\text{-Ps}}$  is at least of the order of  $100\pi a_0^2$  (the reported value<sup>1</sup> of  $\sigma_{o\text{-Ps}}$  is  $1.1 \times 10^3 \pi a_0^2$ ) at a triplet concentration of  $10^{-7}$  and ethane density of 20 amagat at room temperature. It is also possible that the concentration of the molecules in the triplet state is too low (of the order of  $10^{-10}$  or less) to induce changes in  $\lambda_{o\text{-Ps}}$ . It is obvious from Eq. (9) that  $C_T$  depends on several factors such as  $\phi_T$ ,  $\tau_T$ ,  $\epsilon(\omega)$ ,  $L_0(\omega)$ , and  $C$ . Among these factors, the concentration of phosphor molecules  $C$  and the photon flux  $L_0(\omega)$  contribute most to  $C_T$ . The other factors like  $\phi_T$ ,  $\tau_T$ , and  $\epsilon(\omega)$  mainly depend on the type of phosphor molecule and the surroundings. In the following we discuss the experimental conditions of two major factors,  $C$  and  $L_0(\omega)$ , influencing  $C_T$ .

(i)  $L_0(\omega)$ . We had already tried the maximum photon

flux of our uv source with focusing lenses, and still we had not observed any changes in the  $\lambda_{o\text{-Ps}}$ . Unfortunately, we could not directly measure the photon flux of uv source due to lack of a calibrated standard-light source. However, using the known spectral irradiance<sup>13</sup> (average value of  $\sim 15 \mu\text{W cm}^{-2} \text{nm}^{-1}$  between 325 and 375 nm) one can calculate  $L_0(\omega)$  at the excitation wavelengths. Our calculations show an average photon flux of  $\sim 9.6 \times 10^{16}$  photons/sec  $\text{cm}^2$  between 325 and 375 nm at a distance of 50 cm for a collimated beam. A comparison with other reported values of  $L_0(\omega)$  (Refs. 14 and 15) used for similar experiments shows that it is very close to the maximum value used in other experiments. Although we consider the photon flux from our uv source to be sufficiently high based on these considerations, we cannot rule out the possibility of a relatively low population of the excited states in our experiments with gaseous samples. However, we believe that the null result is not due to this possibility of a low photon flux but rather due to a much smaller (than that reported by Brandt<sup>1</sup>) cross section for Ps quenching in collisions with the excited triplet states. Among other numerous tests that we have conducted during the course of these experiments, the following lends additional support to this belief: We have observed with unaided eyes a strong phosphorescence sig-

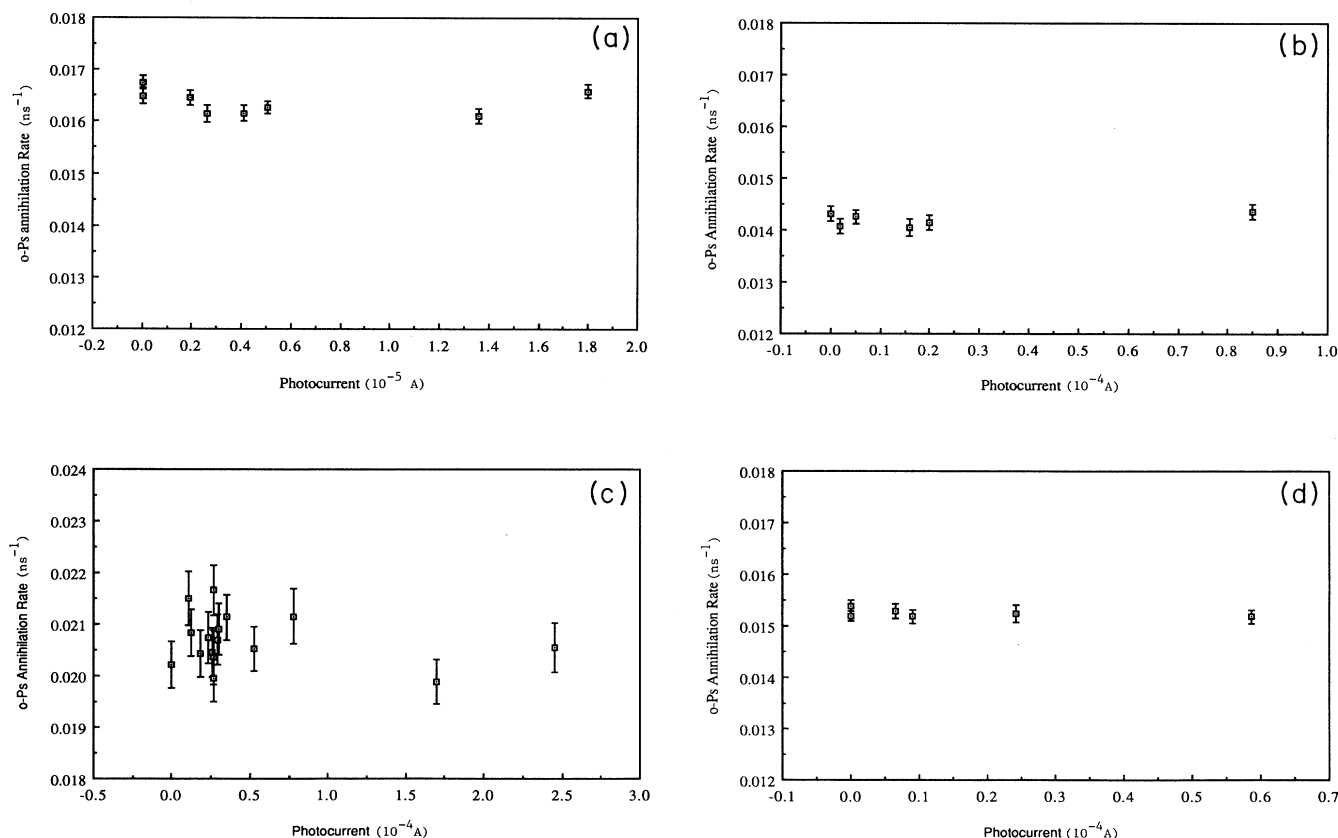


FIG. 7. Pick-off decay rates of  $o$ -Ps vs photocurrent for ethane-benzaldehyde mixtures at different concentrations ( $C$ ) of benzaldehyde in ethane of specified density ( $D$ ). (a)  $C = 3.35 \times 10^{-6}$ ,  $D = 21.4$  amagat; (b)  $C = 5.2 \times 10^{-6}$ ,  $D = 13.5$  amagat; (c)  $C = 3.7 \times 10^{-5}$ ,  $D = 30.9$  amagat; (d)  $C = 2.0 \times 10^{-5}$ ,  $D = 19.3$  amagat.

nal with the solid samples discussed below. This alone proves unambiguously the presence of a high population of the excited triplet states. In spite of such a high  $C_T$ , we have not seen any change in the Ps decay rates.

(ii) *C*. In order to slow down the positrons emitted by the  $^{22}\text{NaCl}$  source and hence have enough Ps formed in the gas sample so that long-lived *o*-Ps component can be separated from the lifetime spectrum we had to keep the total pressure of the mixture at least  $\sim 10$  amagat. This aspect limited our control on *C* allowing the maximum value of only  $\sim 1 \times 10^{-4}$ . We also put a few drops of benzaldehyde liquid directly into the main chamber in order to get the maximum vapor pressure of benzaldehyde vapor at room temperature. This time the benzaldehyde concentration *C* was estimated to be  $9.37 \times 10^{-5}$  from the vapor pressure of the chemical at room temperature,<sup>16</sup> and ethane density was 16.52 amagat. As shown in Table I, neither annihilation rate nor intensity of the *o*-Ps component changed with uv intensity.

#### Test No. 4: Decomposition of benzaldehyde

Though benzaldehyde is known to be a stable chemical under long-time storage, it is possible that the chemical might have been decomposed due to some reasons such as exposure to uv radiation, etc. For this reason, we replaced the existing chemical by sample from a new stock. Two sets of data taken for ethane densities of 19.32 and 19.46 amagat, and fresh-benzaldehyde concentrations of  $2.02 \times 10^{-5}$  and  $4.56 \times 10^{-8}$ , respectively, again showed no change in  $\lambda_{o\text{-Ps}}$ .

#### Test No. 5: Are there any impurities (like oxygen) in the mixture?

It is known that oxygen is a good quencher of triplet-state molecules.<sup>9</sup> For this reason, we installed an oxygen purifier between the mixing chamber and ethane reservoir to remove any possible traces of oxygen from the mixture. A new research-grade ethane reservoir was also connected to the system. We evacuated the whole system for several days at  $\sim 10^{-6}$  torr, prepared a fresh-benzaldehyde-ethane mixture, and again measured the positron lifetime spectrum as functions of uv intensity. Again no significant variation in  $\lambda_{o\text{-Ps}}$  with photocurrent

TABLE I. Annihilation rate and relative intensity of the *o*-Ps component at ethane density of 16.52 amagat and benzaldehyde concentration of  $9.37 \times 10^{-5}$ .

Relative uv intensity (%)	$\lambda_{o\text{-Ps}}$ ( $\text{ns}^{-1}$ )	$I_{o\text{-Ps}}$ (%)
0	$0.01546 \pm 0.00029$	$14.66 \pm 0.15$
10	$0.01563 \pm 0.00029$	$14.59 \pm 0.14$
100	$0.01543 \pm 0.00027$	$15.10 \pm 0.14$

was observed at ethane density of 21.0 amagat and benzaldehyde concentration of  $1.77 \times 10^{-5}$  and also at ethane density of 21.2 amagat and benzaldehyde concentration of  $4.61 \times 10^{-5}$ .

Table II summarizes all 10 sets of data discussed in this section. It shows maximum photocurrent used, ethane density, benzaldehyde concentration, average  $\lambda_{o\text{-Ps}}$ , and average  $I_{o\text{-Ps}}$  for each set.

#### He-benzaldehyde mixtures

As it has been shown above, the uv radiation ( $\lambda \sim 360$  nm) incident on the ethane molecules does not affect *o*-Ps annihilation parameters. However, since we did not observe any variations in  $\lambda_{o\text{-Ps}}$  and  $I_{o\text{-Ps}}$  with photocurrent in ethane-benzaldehyde mixtures, we decided to conduct experiments with helium-benzaldehyde mixtures in order to answer the following questions.

(1) Could ethane molecules quench the excited triplet states  $T^*$  via ethane  $\leftrightarrow T^*$  collisions due to the available inelastic rotational and/or vibrational channels? This possibility did not exist in Brandt's experiments due to the use of helium atoms.

(2) Could we reproduce Brandt's result by performing an experiment for conditions close to those in Brandt's experiment?

However, as the number of  $T^*$  increases with increasing photocurrent, the probability of collisions between  $T^*$  and ethane molecules also increases. Consequently, this may decrease the  $T^*$  concentration by inducing relatively fast nonradiative transitions to the singlet ground state. We have estimated the magnitude of this effect by considering the total number of collisions in the system and the number of  $T^* \leftrightarrow$  ethane molecule collisions and

TABLE II. Summary of the *o*-Ps component results for ethane-benzaldehyde mixtures.

Maximum photocurrent (A)	$D_{\text{C}_2\text{H}_6}$ (amagat)	Benzaldehyde concentration	$\lambda_{o\text{-Ps}}$ ( $\text{ns}^{-1}$ )	$I_{o\text{-Ps}}$ (%)
$1.8 \times 10^{-4}$	21.40	$3.35 \times 10^{-6}$	$0.01637 \pm 0.00014$	$27.57 \pm 0.12^a$
$8.5 \times 10^{-5}$	13.49	$5.21 \times 10^{-6}$	$0.01420 \pm 0.00014$	$17.29 \pm 0.09^a$
$1.5 \times 10^{-4}$	16.89	$5.21 \times 10^{-5}$	$0.01479 \pm 0.00042$	$13.13 \pm 0.19$
$4.8 \times 10^{-3}$	20.73	$3.35 \times 10^{-6}$	$0.01681 \pm 0.00015$	$25.06 \pm 0.11^a$
$2.5 \times 10^{-4}$	30.92	$3.72 \times 10^{-5}$	$0.02066 \pm 0.00045$	$19.50 \pm 0.23$
$5.9 \times 10^{-5}$	19.32	$2.02 \times 10^{-5}$	$0.01524 \pm 0.00014$	$23.33 \pm 0.11^a$
$3.1 \times 10^{-5}$	19.46	$4.56 \times 10^{-8}$	$0.01554 \pm 0.00015$	$14.85 \pm 0.09$
$3.5 \times 10^{-4}$	3.89	$1.24 \times 10^{-4}$	$0.00870 \pm 0.00033$	$3.66 \pm 0.08$
$1.1 \times 10^{-4}$	21.02	$1.77 \times 10^{-5}$	$0.01610 \pm 0.00013$	$16.20 \pm 0.07$
$2.4 \times 10^{-4}$	21.21	$4.61 \times 10^{-5}$	$0.01652 \pm 0.00014$	$15.33 \pm 0.07$

<sup>a</sup>Data taken with different sample of ethane gas, without using oxygen purifier.

found this effect to be negligible. We have also studied this effect further by the following experiment. Helium was chosen in place of ethane. There are no rotational and vibrational excitation channels available for energy loss of helium. Therefore the  $T^*$  deexcitation due to collisions with a helium atom will be much different from that due to collisions with an ethane molecule. Table III contains a summary of several measurements made for two different helium-benzaldehyde mixtures as functions of photocurrent intensities. Neither  $\lambda_{o\text{-Ps}}$  nor  $I_{o\text{-Ps}}$  changes with photocurrent. Therefore the obvious differences between these two systems, namely ethane $\leftrightarrow T^*$  and helium $\leftrightarrow T^*$ , have no observable effect on the annihilation parameters.

To answer the second question we designed and built an experimental chamber which had the same size and shape as the one used for Brandt's experiment. Positron lifetime spectra were obtained in helium-benzaldehyde mixture containing helium density and benzaldehyde concentration identical to one of the mixtures used by Brandt<sup>1</sup> (1 atom of He at 295 K, and benzaldehyde concentration of  $1.3 \times 10^{-3}$ ). We also used the same type of uv source (Hg-arc lamp). Lifetime spectra were collected so that each spectrum contained total counts  $\sim 0.8 \times 10^6$ . (Brandt's data had only  $\sim 10^4$  total counts under the lifetime spectrum.) For the analysis of the lifetime spectra, we used standard POSITRONFIT analysis as well as the method used by Brandt. The latter involves only calculating the area under the lifetime spectrum for times greater than a certain value  $t_c$  to separate the  $o\text{-Ps}$  component from the two other shorter components. Our results showed that uv radiation did not induce any changes in  $o\text{-Ps}$  annihilation parameters. For all photocurrents,  $\lambda_{o\text{-Ps}} = 0.0075 \pm 0.0003 \text{ ns}^{-1}$ . In conclusion, we could not reproduce Brandt's results.

#### Solid samples

With the photomagnetic molecules in gas phase we could not observe any uv-induced changes in  $\lambda_{o\text{-Ps}}$  and  $I_{o\text{-Ps}}$ . Therefore it is very important to verify that there existed excited triplet states of the photomagnetic molecules in the main chamber. This can be done by detecting phosphorescence from the photomagnetic molecules. However, detecting phosphorescence right from the main chamber turned out to be inefficient due to a relatively small solid angle at the exit window of the main chamber. Therefore, as an alternative plan, we conducted experiments with several solid samples whose phosphorescent

deexcitation is known to be in the visible range ( $\sim 500 \text{ nm}$ ) at 77 K.<sup>4</sup> The phosphorescent deexcitation from these solid samples at 77 K could be observed by unaided eyes in a dark room. Samples were in the form of powder, and they were spread over the  $^{22}\text{Na}$  source on top of a copper cold finger that was in contact with liquid nitrogen. The copper rod of this cold finger was covered by a double-wall test tube to prevent air condensation. Thickness of the sample was approximately 1 mm in every case. One of the samples was pure benzophenone powder, while the others were silica gels with benzophenone and 2-bromonaphthalene as the photomagnetic molecules. The lichrospher silicas used for this experiment have a mean particle size of  $10 \mu\text{m}$  and mean pore size of  $60 \text{ \AA}$ . The samples were prepared by Exxon Research Lab by the adsorption of phosphor molecules pentane, etc., which yields surface concentrations for the phosphor molecules of  $\sim 10^{-5}$  moles per gram of silica. Further details of sample preparation are given elsewhere.<sup>4</sup> Throughout the measurements with these solid samples, phosphorescent deexcitation was detected thus confirming the presence of the excited triplet states. Table IV shows our results from a series of measurements with the solid samples. With the benzophenon powder, both lifetime and Doppler broadening measurements showed no uv-induced changes at 77 K, which is in good agreement with our measurements with the gas samples. No changes in  $\lambda_{o\text{-Ps}}$  and  $I_{o\text{-Ps}}$  were observed due to uv irradiance of the silica gel samples. However, a considerable temperature effect on  $I_{o\text{-Ps}}$  is observed with the silica gel benzophenone (SG-BP) sample between 77 K and 295 K. The large increase in  $I_{o\text{-Ps}}$  at 295 K is possibly due to the powder effect and due to defects which can change Ps formation yields at different temperatures. A slight change in  $I_{o\text{-Ps}}$ 's with SG-BP sample at 77 K could also arise due to uv radiation heating of the sample.

From the results shown in Table IV, it is clear that there is no observable effect of ortho-to-para Ps conversion due to  $o\text{-Ps} \leftrightarrow T^*$  interactions.

#### Ethane-oxygen mixtures

We have so far populated the excited triplet states from the ground singlet states by uv radiation. However, the ground state of an  $\text{O}_2$  molecule, which is well known to be an efficient  $o\text{-Ps}$  quencher, is a triplet. The first- and second-excited states are singlets which are separated by 0.977 and 1.627 eV from the ground state, respectively. The results of  $o\text{-Ps}$  quenching in oxygen are well known

TABLE III. Annihilation rate and intensity of the  $o\text{-Ps}$  components in helium-benzaldehyde mixtures.

Photocurrent ( $10^{-3} \text{ A}$ )	$D_{\text{He}}$ (amagat)	Benzaldehyde concentration	$\lambda_{o\text{-Ps}}$ ( $\text{ns}^{-1}$ )	$I_{o\text{-Ps}}$ (%)
0	9.52	$2.32 \times 10^{-5}$	$0.00973 \pm 0.00032$	$2.95 \pm 0.06$
0.5	9.52	$2.32 \times 10^{-5}$	$0.01166 \pm 0.00123$	$2.79 \pm 0.16$
5.0	9.52	$2.32 \times 10^{-5}$	$0.00973 \pm 0.00029$	$2.88 \pm 0.05$
0	15.69	$6.03 \times 10^{-6}$	$0.01040 \pm 0.00048$	$7.56 \pm 0.17$
0.5	15.69	$6.03 \times 10^{-6}$	$0.01046 \pm 0.00024$	$7.58 \pm 0.08$

TABLE IV. Results for solid samples.

Sample	Relative uv intensity (%)	$\lambda_{o-Ps}$ (ns <sup>-1</sup> )	$I_{o-Ps}$ (%)	S parameter	T (K)
Benzophenone	0	0.9939±0.0166	5.47±0.17	0.545±0.001	77
Benzophenone	10	0.9959±0.0133	5.43±0.13		77
Benzophenone	100	0.9859±0.0137	5.44±0.14	0.546±0.001	77
SG-BP <sup>a</sup>	0	0.5685±0.0313	5.01±0.64		77
SG-BP <sup>a</sup>	100	0.5993±0.0123	6.90±0.23		77
SG-BP <sup>a</sup>	0	0.5320±0.0099	17.06±0.75		295
SG-BP <sup>a</sup>	100	0.5452±0.0048	17.95±0.25		295
SG-BN <sup>b</sup>	0	0.6113±0.0289	5.35±0.57		77
SG-BN <sup>b</sup>	100	0.5932±0.0133	5.26±0.17		77

<sup>a</sup>SG-BP=silica gel with benzophenone.

<sup>b</sup>SG-BN=silica gel with 2-bromonaphthalene.

through a number of previous measurements.<sup>17</sup> The main purpose of this experiment with ethane-oxygen mixtures was to provide additional checks on our experimental system by measuring  $\lambda_{o-Ps}$  with oxygen concentration ( $C_{O_2}$ ) to obtain  $o$ -Ps conversion rate  $w(o \rightarrow p)$  and the scattering cross section ( $\sigma_{o-Ps}$ ) for  $o$ -Ps spin conversion in collisions with  $O_2$ . As we discuss in the following, however, these experiments have provided some interesting new results.

In the present experiment,  $o$ -Ps lifetime has been measured in ethane-oxygen mixtures at various oxygen concentrations up to  $\sim 0.15$ . The total density of the mixture was maintained constant at 14.7 amagat. A constant total density of this order in the chamber assures, to at least first order, that there are no systematic errors in the resolution of especially the shortest-lived (lifetime  $\sim 0.2$  ns) and the intermediate (lifetime  $\sim 0.8$  ns) components. This is so because the shortest component represents contributions from the annihilations of parapositronium and of positrons reaching the walls of the metallic chamber. Significant changes in the total density of the mixture in the chamber could result in systematic changes in the lifetime of the shortest component due to density-dependent variations in the positron stopping power. This could then influence the relative intensity of the intermediate component. Since we have been interested in these experiments with both the longest-lived  $o$ -Ps component and the intermediate "free positron" component, care was taken to eliminate any systematic errors in the intermediate component by maintaining a constant total density in the chamber. Figure 8 shows the results for  $\lambda_{o-Ps}$  as a function of  $O_2$  concentration ranging from 0 to 0.15.  $\lambda_{o-Ps}$  increases linearly with  $O_2$  concentration, and this behavior provides  $W(o \rightarrow p) = 0.35 \text{ ns}^{-1}$  and  $\sigma_{o-Ps}$ ,  $(1.07 \pm 0.05) \times 10^{-19} \text{ cm}^2$ , in excellent agreement with the previous results.<sup>17</sup> The processes involved in  $o$ -Ps  $\leftrightarrow O_2$  interaction include (i) elastic direct scattering and elastic exchange scattering, in which the electrons of the  $o$ -Ps atom and  $O_2$  are exchanged and  $O_2$  remains in the triplet ground states, and (ii) inelastic scattering in which an energetic positron/positronium excites  $O_2$  into one of the excited states. From the  $\lambda_{o-Ps}$  data, the dominant process responsible for the  $o$ -Ps quenching is believed to be ortho-to-para Ps conversion via elastic exchange interac-

tion between  $o$ -Ps and  $O_2$ . The value of  $\sigma_{o-Ps}$  obtained from our analysis agrees well with the cross section for the elastic conversion measured in several other experiments. It, therefore, supports the above argument. The annihilation rate of free positrons  $\lambda_f$  is expected not to change with  $O_2$  concentration. The results obtained for  $\lambda_f$  are shown in Fig. 9, and they show no significant change in  $\lambda_f$  with  $O_2$  concentration.

We consider the decay scheme of Ps in ethane-oxygen mixture which is shown in Fig. 10. All of the possible channels for Ps disappearance are included in this scheme. In this, system the solutions of well-known population equations can be written as the following:<sup>18</sup>

$$\begin{aligned}
 n_p(t) &= Ae^{-\lambda_1 t} + Be^{-\lambda_2 t}, \\
 n_o(t) &= Ce^{-\lambda_1 t} + De^{-\lambda_2 t}, \\
 n_f(t) &= \frac{\lambda_o(B+D)}{\lambda_f - \lambda_2} (e^{-\lambda_2 t} - e^{-\lambda_f t}) + n_f(0)e^{-\lambda_f t}, \\
 n_m(t) &= \frac{\lambda_c \chi(B+D)}{\lambda_m - \lambda_2} (e^{-\lambda_2 t} - e^{-\lambda_m t}) + n_m(0)e^{-\lambda_m t}.
 \end{aligned} \tag{18}$$

The decay rates  $\lambda_1$  (with + sign) and  $\lambda_2$  (with - sign) are given by

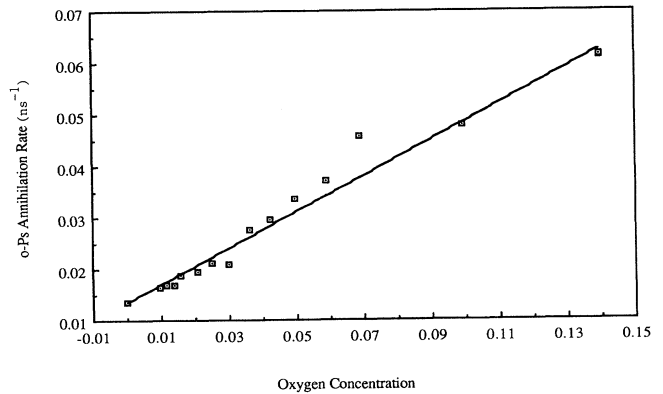


FIG. 8.  $o$ -Ps pick-off decay rate vs oxygen concentration in ethane-oxygen mixtures at a constant total density of 14.7 amagat. The statistical error bars fall within the data points.

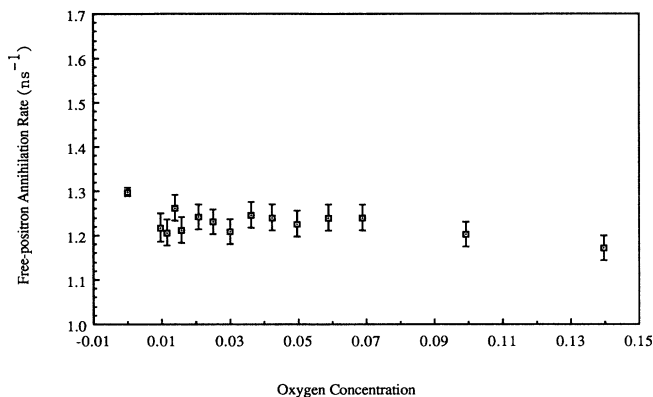


FIG. 9. Free positron decay rate vs oxygen concentration in ethane-oxygen mixtures at a constant total density of 14.7 amagat.

$$\lambda_{1,2} = 2\omega\chi + \frac{\lambda_s}{2} + \frac{\lambda_t}{2} + \lambda_p + \lambda_o + \lambda_c\chi \pm \left[ 4\omega^2\chi^2 + \omega\chi\lambda_s + \frac{\lambda_s^2}{4} + \frac{\lambda_t^2}{4} - \frac{\lambda_s\lambda_t}{4} - \omega\chi\lambda_t \right]^{1/2},$$

$$A = \frac{\lambda_s + \lambda_p + \lambda_o + \lambda_c\chi - \lambda_2}{\lambda_1 - \lambda_2} n_p(0),$$

$$B = \frac{\lambda_1 - (\lambda_s + \lambda_p + \lambda_o + \lambda_c\chi)}{\lambda_1 - \lambda_2} n_p(0),$$

$$C = \frac{\lambda_t + \lambda_p + \lambda_o + \lambda_c\chi - \lambda_2}{\lambda_1 - \lambda_2} n_o(0),$$

$$D = \frac{\lambda_1 - (\lambda_t + \lambda_p + \lambda_o + \lambda_c\chi)}{\lambda_1 - \lambda_2} n_o(0).$$

Here  $n_m$  = number of Ps-molecule compounds at time  $t$ ,  $\lambda_s$  = annihilation rate of  $p$ -Ps (singlet),  $\lambda_t$  = annihilation rate of  $o$ -Ps (triplet),  $\lambda_p$  = pick-off annihilation rate,  $\omega$  = Ps conversion rate,  $\chi$  = triplet concentration,  $\lambda_f$  = annihilation rate of free positrons,  $\lambda_m$  = annihilation rate of positrons in Ps-molecule compound,  $\lambda_o$  = Ps oxidation rate,  $\lambda_c$  = compound formation rate.

Figure 11 shows the intensity  $I_{o-Ps}$  as a function of oxygen concentration which decreases with increasing oxygen concentration. When the ortho-to-para conversion rate is higher than the annihilation rate of  $p$ -Ps, the extent of ortho-to-para conversion can be compensated by an inverse conversion of para-to-ortho, thus the net effect appears as a simple slowing down of  $o$ -Ps. If the conversion rate is lower than the annihilation rate [which happens to be the case,  $W(o \rightarrow p) \sim 0.35 \text{ ns}^{-1}$ ], most of the  $p$ -Ps atoms do not survive to convert to  $o$ -Ps. In other words, ortho-to-para occurs long after all of the original  $p$ -Ps has annihilated. This will result in a net decrease in  $I_{o-Ps}$ . Our experimental data agree with this argument showing a decrease in  $I_{o-Ps}$ .

If the presence of  $O_2$  in the ethane-oxygen mixtures

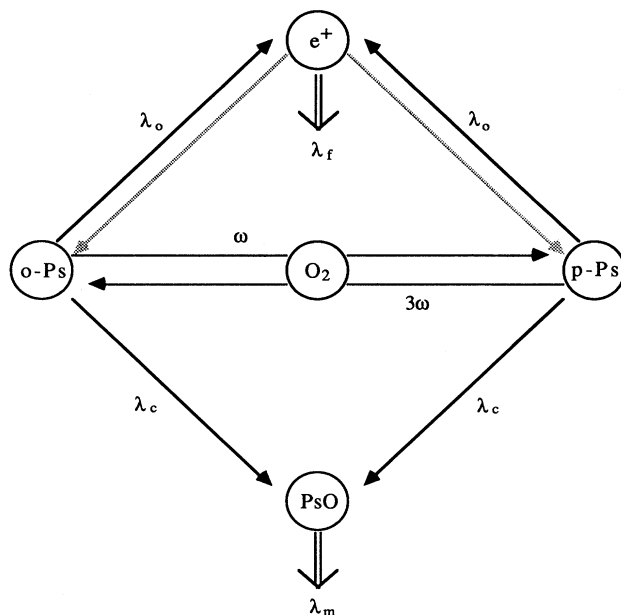


FIG. 10. The decay channels considered for Ps decay in ethane-oxygen mixtures.

were only promoting ortho-to-para conversion of the Ps atoms, the intensity of the intermediate “free positron” component should not vary with oxygen concentration. On the other hand, positronium quenching via additional channels, like those involving Ps oxidation and Ps-molecule compound formation, can significantly affect the intensity of the intermediate component especially when the Ps decay rate for these additional quenching channels is indistinguishable from the decay rate of the “free” state. We show in Fig. 12 the relative intensity of the intermediate lifetime component (decay rate  $\lambda_f$ , which has been shown in Fig. 9, to be independent of oxygen concentration) as a function of oxygen concentration in ethane-oxygen mixtures. The lifetime of the intermediate component ( $\sim 0.8 \text{ ns}$ ) is several times longer than the lifetime (0.25 ns) of the shortest-lived component. As

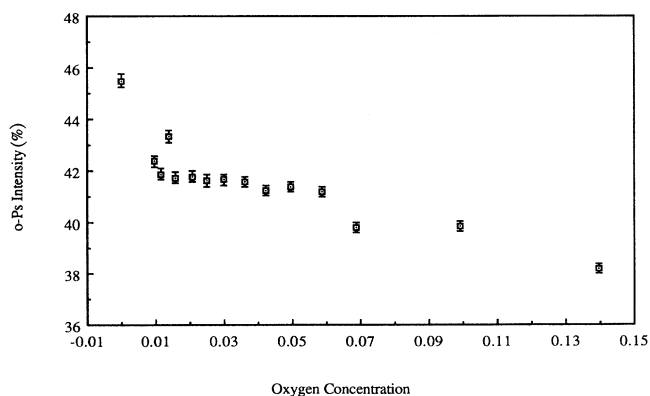


FIG. 11. Relative intensity of the  $o$ -Ps component vs oxygen concentration in ethane-oxygen mixtures.

stated earlier, this latter component represents contributions from the annihilations of *p*-Ps and of positrons reaching the walls of the metallic chamber. Since we were primarily interested in the *o*-Ps component, whose lifetime ranged from approximately 16 to 70 ns for the entire range of oxygen concentrations, the spectrometer resolution (FWHM=0.4 ns) is considered very good; all three lifetime components (lifetimes=0.25, 0.8, and 16–70 ns) are well resolved. We took precautions to ensure that the shortest-lived component did not contribute to systematic errors in the determination of the relative intensity of the intermediate component, which turned out to be an important result of this investigation. For example, the lifetime of the shortest component was monitored carefully. It turned out to be essentially independent of oxygen concentration and therefore the relative changes in the intensity of the intermediate component, shown in Fig. 12, are “free” from systematic errors due to possible correlations between the shortest lifetime and the intensity of the intermediate component. The intensity of the intermediate component is remarkably sensitive to the concentration of oxygen in ethane-oxygen mixtures; it changes by about 40% for oxygen concentrations ranging from 0 to 0.15. Based on the above discussion and additional supporting results discussed below, we suggest that the observed increase in this intensity arises due to contributions to the intermediate component from Ps oxidation and/or Ps-molecule compound formation. We, therefore, characterize the intermediate lifetime component as representing contributions from annihilations of free positrons and of *o*-Ps via Ps oxidation and/or Ps-molecule compound formation (decay rate  $\lambda_m \sim \lambda_f$ ).

Therefore, both of the processes, oxidation of Ps and Ps-molecule compound formation, will give rise to an increase in  $I_f$ . From Eq. (18)  $I_f$  is given by

$$I_f = n_f(0) + n_m(0) - \frac{\lambda_c \chi (B + D)}{\lambda_m - \lambda_2} - \frac{\lambda_o (B + D)}{\lambda_f - \lambda_2} \quad (20)$$

The curve shown in Fig. 12 was obtained by fitting Eq. (20) to the  $I_f$  data and it corresponds to  $\lambda_c = 1.44 \pm 0.5 \text{ ns}^{-1}$ ,  $\lambda_m = 0.66 \pm 0.1 \text{ ns}^{-1}$ , and  $\lambda_o = 0.16 \pm 0.03 \text{ ns}^{-1}$ . The annihilation rates of the Ps-molecule compound ( $\lambda_m$ ) in various liquids have been reported to be  $1.0 \sim 2.0 \text{ ns}^{-1}$ .<sup>18,19</sup> This agrees reasonably well with our value of  $\lambda_m$  for gaseous ethane. The value of  $\lambda_c$  and  $\lambda_o$  in gaseous media are not available in the literature. These results suggest Ps-molecule compound formation as well as the occurrence of Ps oxidation in ethane-oxygen mixtures. However, each of these reactions involves a certain threshold energy. Consequently, in order for such a reaction to proceed the kinetic energy of the Ps atom must meet specific requirements that are discussed below. Only a few experimental values for Ps-molecule compound formation threshold energies are available in the literature.<sup>20</sup> For example, several Ps affinities (in eV) are as follows:

PsO	PsOH	PsF	PsCl
$2.2 \pm 0.05$	$< 1.5$	$2.9 \pm 0.5$	$2.0 \pm 0.5$

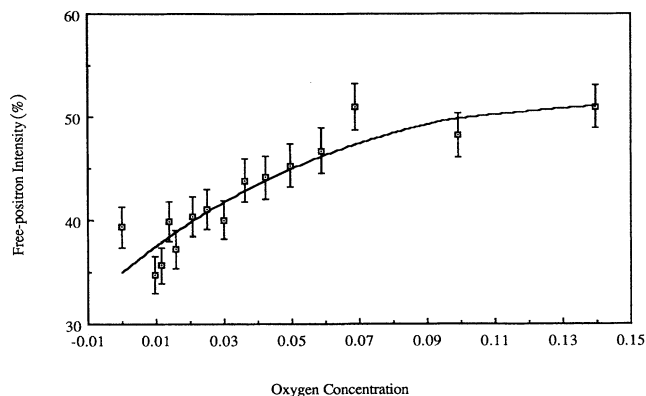


FIG. 12. Relative intensity of the intermediate component vs oxygen concentration in ethane-oxygen mixtures.

For the formation of a stable Ps-molecule compound in a reaction of the type



the dissociation energy of the Ps compound ( $D_{\text{PsA}}$ ) must be positive. Moreover, the minimum energy that must be supplied by the Ps atom to facilitate the reaction is determined by  $(D_{\text{AB}} - D_{\text{PsA}})$ , where  $D_{\text{AB}}$  is the dissociation energy of the compound AB. If  $D_{\text{AB}} - D_{\text{PsA}} > kT$  (thermal energy), the reaction cannot take place with Ps atoms having kinetic energy  $= kT$ . In the case  $D_{\text{AB}} - D_{\text{PsA}} < 0$ , on the other hand, the reaction can also proceed at thermal energies. In ethane-oxygen mixtures, where  $D_{\text{PsA}} = D_{\text{PsO}} = 2.2 \text{ eV}$ , and  $D_{\text{AB}} = D_{\text{O}_2} = 5.17 \text{ eV}$ , the process in Eq. (21) becomes possible when one considers “hot” (not thermal) Ps atoms having kinetic energy in the range  $(5.17 - 2.2) \text{ eV} < E_{\text{Ps}} < 6.8 \text{ eV}$ .

Ps oxidation process in  $\text{O}_2$  gas can be expressed by



The electron affinity of  $\text{O}_2$  for the formation of  $\text{O}_2^-$  is only 0.45 eV.<sup>16</sup> Therefore if we consider only thermal Ps interacting with an  $\text{O}_2$  molecule, then the process in Eq. (22) is not possible due to a high binding energy of Ps (6.8 eV). However, to account for the observed change in  $I_f$ , we assume that the oxidation of “hot” (not thermal) *o*-Ps atoms by  $\text{O}_2$  molecules proceeds via simple electron transfer. This assumption is valid only when the kinetic energy of the positronium atom lies in the range  $(6.8 - 0.45) \text{ eV} < E_{\text{Ps}} < 6.8 \text{ eV}$ . A similar Ps oxidation effect has previously been observed in several aqueous solutions.<sup>19,21</sup>

## V. CONCLUSIONS

In summary, we have presented results from a study of the positronium interactions with the triplet states of photomagnetic molecules in the gas phase as well as in the solid phase. Based on the results of the *o*-Ps annihilation parameters, measured in a number of different samples under varying experimental conditions, we believe

that the *o*-Ps spin conversion cross section is not large enough to induce significant changes in the *o*-Ps decay rate and/or its relative intensity at such low concentrations of the photomagnetic molecules ( $\sim 10^{-8}$  to  $\sim 10^{-4}$ ) as reported earlier.<sup>1,14</sup> A number of important tests were performed to eliminate any possible sources of errors and hence to resolve this discrepancy. From the results of the tests we conclude that there are no noticeable effects of  $\text{Ps} \leftrightarrow T^*$  interaction on *o*-Ps annihilation parameters at phosphor concentrations ranging from  $\sim 10^{-8}$  to  $\sim 10^{-4}$ . Consequently, *o*-Ps spin conversion cross section should not be as large as previously reported. We have recently learned of an independent study by Diehl and Schrader<sup>22</sup> in which these authors also have made exhaustive attempts to reproduce Brandt's results. Diehl and Schrader too cannot reproduce Brandt's data. They report that the positron lifetime spectra measured for irradiated benzene under the conditions of the earlier Brandt's experiments show no effect; even the spectra measured under new conditions of temperature, of light-shuttering times, and of several different geometrical arrangements show no effect. These authors have also investigated this phenomenon with more phosphors (anthracene and benzophenone in methylcyclohexane glasses) and have seen no such effect as that reported by Brandt.

For an oxygen molecule,  $\sigma_{o\text{-Ps}}$  is obtained to be

$1.07 \times 10^{-19} \text{ cm}^2$ , which is in excellent agreement with the previous results. The annihilation rate of free positrons  $\lambda_f$  does not vary with  $\text{O}_2$  concentration in  $\text{C}_2\text{H}_6\text{-O}_2$  mixtures as expected. The intensity of the *o*-Ps component  $I_{o\text{-Ps}}$  decreases with increasing oxygen concentration, which implies that the ortho-to-para conversion rate is lower than the *p*-Ps annihilation rate. The intensity of the free positron component ( $I_f$ ) is expected not to vary with oxygen concentration in the absence of processes involving Ps oxidation and Ps-molecule compound formation. However,  $I_f$  data show as much as  $\sim 40\%$  increase with  $\text{O}_2$  concentration in ethane-oxygen mixtures. This increase is discussed in terms of Ps oxidation and Ps-molecule compound formation. Considerations of the reaction energies suggest reactions between "hot" (non-thermal) Ps and  $\text{O}_2$  molecules in the mixtures.

#### ACKNOWLEDGMENTS

We thank Dr. J. M. Drake, Exxon Research and Engineering Company, for kindly providing silica gel samples. This research was supported by grants from the Robert A. Welch Foundation (No. Y-1013), Houston, Texas and the Research Enhancement Program of the University of Texas at Arlington.

\*Present address: Korea Standards Research Institute, Taejon, Korea.

†Present address: Department of Physics, Grambling State University, Grambling, LA 71245.

‡Present address: Department of Physics, University of North Texas, Denton, TX 76203.

<sup>1</sup>W. Brandt and D. Spektor, *Phys. Rev. Lett.* **38**, 595 (1977).

<sup>2</sup>S. C. Sharma, J. D. McNutt, A. Eftekhari, and Y. J. Ataiyan, *Can. J. Phys.* **60**, 610 (1982).

<sup>3</sup>S. C. Sharma, S. D. Hyatt, M. H. Ward, and C. A. Dark, *J. Phys. B* **18**, 3245 (1985).

<sup>4</sup>J. M. Drake, P. Levitz, J. Klafter, N. J. Turro, K. S. Nitsche, and K. F. Cassidy, *Phys. Rev. Lett.* **61**, 865 (1988).

<sup>5</sup>C. I. Eom, Ph.D. dissertation, University of Texas at Arlington, 1989 (unpublished).

<sup>6</sup>P. Kirkegaard and M. Eldrup, *Comput. Phys. Commun.* **7**, 401 (1974).

<sup>7</sup>S. C. Sharma, in *Positron and Positronium Chemistry*, edited by D. M. Schrader and Y. C. Jean (Elsevier, New York, 1988), p. 193.

<sup>8</sup>S. C. Sharma and J. D. McNutt, *Phys. Rev. A* **18**, 1426 (1978).

<sup>9</sup>T. Vo-Dinh, *Chemical Analysis* (Wiley-Interscience, New York, 1984), Vol. 68.

<sup>10</sup>N. J. Turro, *Modern Molecular Photochemistry* (Benjamin/Cummings, New York, 1978).

<sup>11</sup>S. C. Sharma, in *Positron Annihilation Studies of Fluids*, edited by S. C. Sharma (World Scientific, Singapore, 1988).

<sup>12</sup>S. C. Sharma, J. D. McNutt, A. Eftekhari, and R. A. Hejl, *J. Chem. Phys.* **75**, 1226 (1981).

<sup>13</sup>Oriel report, 1985 (unpublished).

<sup>14</sup>W. Brandt and P. Kliauga, *Phys. Rev. B* **14**, 884 (1976).

<sup>15</sup>U. Bruhlmann, M. Nonella, P. Russegger, and J. R. Huber, *Chem. Phys.* **81**, 439 (1983).

<sup>16</sup>*Handbook of Chemistry and Physics* (CRC, Boca Raton, FL, 1988).

<sup>17</sup>M. Kokimoto, T. Hyodo, and T. B. Chang, *J. Phys. B* **23**, 589 (1990), and references therein.

<sup>18</sup>J. D. McGervey, in *Positron Annihilation*, edited by A. T. Stewart and L. O. Roelling (Academic, New York, 1967), p. 143.

<sup>19</sup>V. I. Goldanskii, in *Positron Annihilation* (Ref. 18), p. 183.

<sup>20</sup>D. M. Schrader, in *Positron and Positronium Chemistry* (Ref. 7), p. 27.

<sup>21</sup>H. J. Ache, *Angew. Chem. Int. Ed. Eng.* **11**, 179 (1972).

<sup>22</sup>D. A. Diehl and D. M. Schrader, in *Photomagnetic Quenching*, Proceedings of the Third International Workshop on Positron and Positronium Chemistry, Milwaukee, Wisconsin, edited by Y. C. Jean (World Scientific, Singapore, 1990), p. 384.